

# Rationally Designed Eugenol-Based Chain Extender for Self-Healing Polyurethane Elastomers

Uk-Jae Lee,<sup>#</sup> Se-Ra Shin,<sup>#</sup> Heewon Noh,<sup>#</sup> Han-Bit Song, Junyeob Kim, Dai-Soo Lee,<sup>\*</sup> and Byung-Gee Kim<sup>\*</sup>



Cite This: *ACS Omega* 2021, 6, 28848–28858



Read Online

ACCESS |



Metrics & More

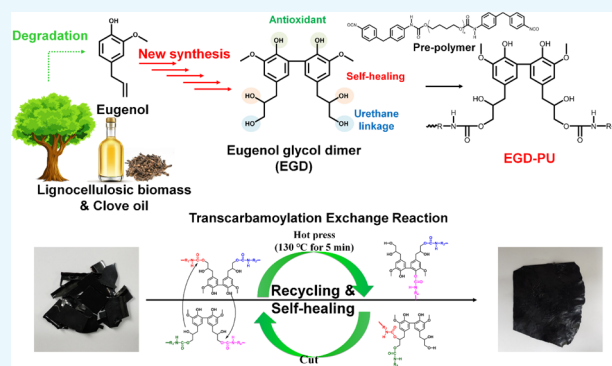


Article Recommendations



Supporting Information

**ABSTRACT:** Bio-based polyurethane (PU) has recently drawn our attention due to the increasing interest in sustainability and the risks involved with petroleum depletion. Herein, bio-based self-healing PU with a novel polyol, *i.e.*, eugenol glycol dimer (EGD), was synthesized and characterized for the first time. EGD was designed to have pairs of primary, secondary, and aromatic alcohols, which all are able to be involved in urethane bond formation and to show self-healing and antioxidant effects. EGD was incorporated into a mixture of the prepolymer of polyol (tetramethylene ether glycol) and 4,4'-methylene diphenyl diisocyanate to synthesize PU. EGD-PU showed excellent self-healing properties (99.84%), and it maintained its high self-healing property (84.71%) even after three repeated tests. This dramatic self-healing was induced through transcarbamoylation by the pendant hydroxyl groups of EGD-PU. The excellent antioxidant effect of EGD-PU was confirmed by 2,2-diphenyl-1-picrylhydrazyl analysis. Eugenol-based EGD is a promising polyol chain extender that is required in the production of bio-based, self-healing, and recyclable polyurethane; therefore, EGD-PU can be applied to bio-based self-healable films or coating materials as a substitute for petroleum-based PU.



## INTRODUCTION

In polyurethane (PU) synthesis, there has been a growing push in recent years to replace petrochemical polyol and employ renewable resources by increasing levels of biomass content. In this context, lignocellulosic biomass-derived polyols have been developed as ways to produce green polyurethane.<sup>1–5</sup>

PU is a highly versatile polymer that can be used in a wide variety of applications including coating, adhesives, elastomers, insulators, elastic fibers, foams, and integral skins.<sup>6</sup> Urethane linkage ( $-\text{NH}-(\text{C}=\text{O})-\text{O}-$ ), *i.e.*, the linkage of a carbamate synthesized by the addition reaction between isocyanate and alcohol groups, is a common feature in all PUs.<sup>7</sup> Since the polyols providing the alcohol groups have conventionally been obtained from petrochemical crude oils and coals, they raise a serious environmental issue regarding depletion of natural resources;<sup>8,9</sup> therefore, efforts have gone toward developing new technologies for the commercial production of bio-based polyols from biomass or its degradation byproducts and for green PU synthesis.<sup>1,8–12</sup> In addition, the physical and chemical properties of PU can be readily adjusted by changing synthetic processes or varying the compositions of the constituting monomers (diisocyanates and polyols).

Lignin, the most abundant aromatic polymers in lignocellulose, or its destructed oligomer products, when incorporated into PU, can increase the content of green carbon source from

biomass<sup>2</sup> and provide enhanced performance scores for PU including enhanced cross-linking density,<sup>3</sup> antioxidant properties,<sup>4</sup> mechanical strength,<sup>5</sup> and thermal stability.<sup>2,9,13</sup> However, the utilization of lignin as a PU polyol is limited by its high poly-dispersity, low solubility, and steric hindrance;<sup>14</sup> therefore, several studies have attempted to develop lignin-derived PUs.<sup>1,15</sup> In one example, bio-based di-vanillin PU showed enhanced stiffness as the aromatic ring and irreversible covalent bonds provide structural stability.<sup>1</sup> However, it lacked a self-healing property and was vulnerable to microcracks. To achieve self-healing, diverse reversible covalent networks have been introduced into PUs.<sup>16–18</sup> The resulting products have an extended life span, improved reliability during applications, and reduced content of polymer wastage.<sup>19</sup> Therefore, dynamic covalent chemistry has been investigated for its ability to enhance the self-healing of PUs for applications in materials for usage in implanted medical devices, aerospace appliances, and protective coatings.<sup>20–22</sup> For example, the reversible disulfide

Received: July 16, 2021

Accepted: September 30, 2021

Published: October 21, 2021



## Scheme 1. Synthesis of Eugenol Glycol Dimer (EGD) from Eugenol

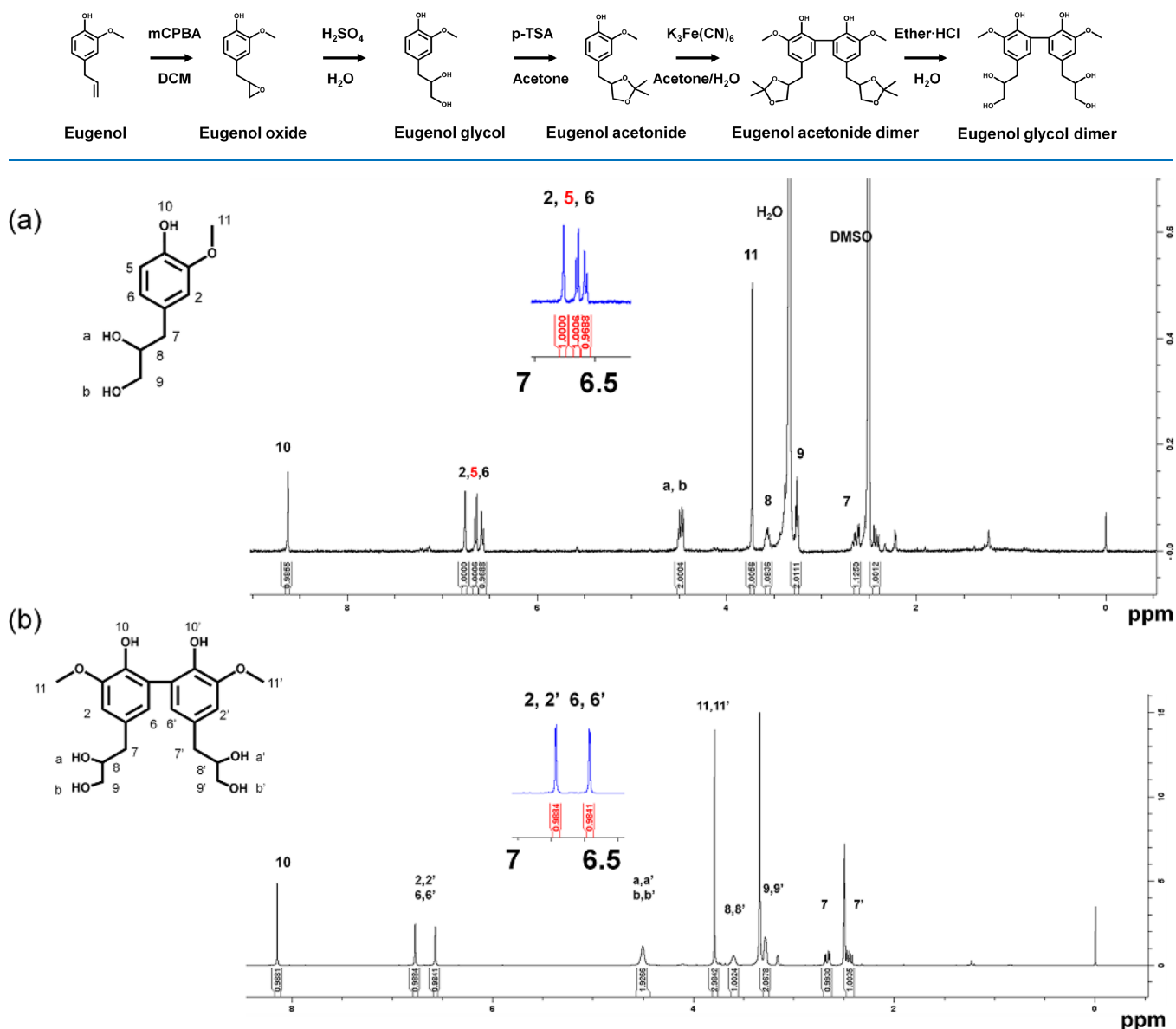


Figure 1. <sup>1</sup>H-NMR of (a) eugenol glycol and (b) eugenol glycol dimer (EGD).

bond and hydrogen bonding in PU contributed to the self-healing in flexible electronics.<sup>23</sup> The dynamic disulfide bond-incorporated PU showed an excellent performance in 3D printing with its repeatable self-healing and high stretchability.<sup>24</sup> PUs can incorporate dynamic covalent reactions, including imine formation,<sup>25</sup> boronate ester exchange,<sup>26</sup> disulfide exchange,<sup>27</sup> Diels–Alder,<sup>28</sup> and amine/urea exchange reactions.<sup>29</sup> Transcarbamoylation represents another reversible exchange, as the urethane bond can undergo the exchange reactions for self-healing.<sup>30,31</sup> Unfortunately, the reversible exchange reaction typically requires high temperature (>200 °C) or a catalyst to support self-healing, but rich phenol or hydroxyl groups promote the reaction under mild heating in the absence of the catalysts.<sup>31–33</sup> As a result, we hypothesized that introducing more hydroxyl groups into the lignin derivatives might be an important factor for designing a new polyol chain extender of self-healing PU.

Eugenol, which is mainly obtained in nature from clove oils,<sup>34</sup> can be obtained in large quantities as a byproduct of the thermal decomposition of lignin.<sup>35</sup> Eugenol by itself fails to meet the requirements of a PU chain extender, as it lacks the difunctional hydroxyl groups that react with the diisocyanate group. Its alkenyl group can be modified into two or more reactive hydroxyl groups through epoxidation–trimerization,<sup>36</sup> or copolymerization with a terminal thiol group-modified oligomer<sup>37</sup> and soybean oil.<sup>38</sup> Herein, eugenol glycol dimer (EGD), a novel eugenol-based PU chain extender, was designed to supply symmetrical hydroxyl groups (Scheme 1). Since EGD has pairs of primary, secondary hydroxyl, and phenolic groups, such a polyol might provide proper carbamate linkages, self-healing,<sup>31,33</sup> and antioxidant properties into the PUs.<sup>39–41</sup> Eugenol glycol was obtained via epoxidation and hydroxylation.<sup>42</sup> While eugenol was dimerized with oxidative coupling reagent,<sup>43</sup> eugenol glycol does not directly undergo dimerization. It was believed that diol in eugenol glycol might

## Scheme 2. Synthesis of Polyurethane with Control Hexanediol (HD) and Eugenol Glycol Dimer (EGD)

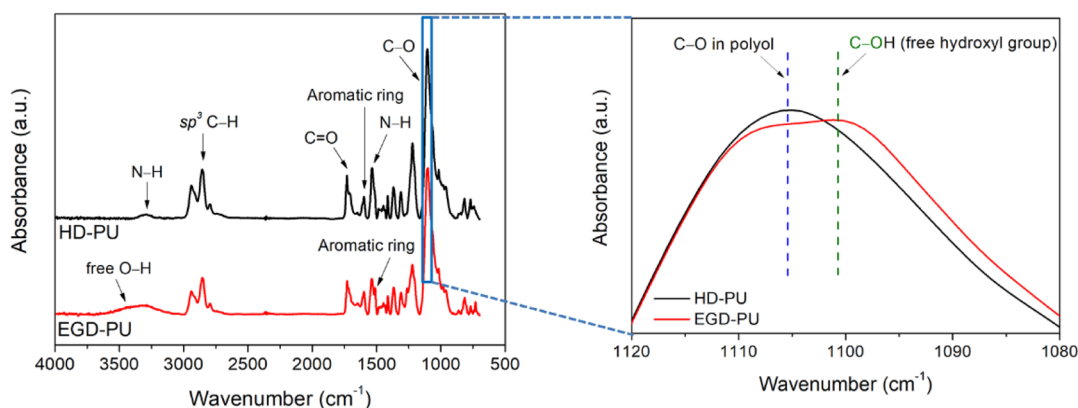
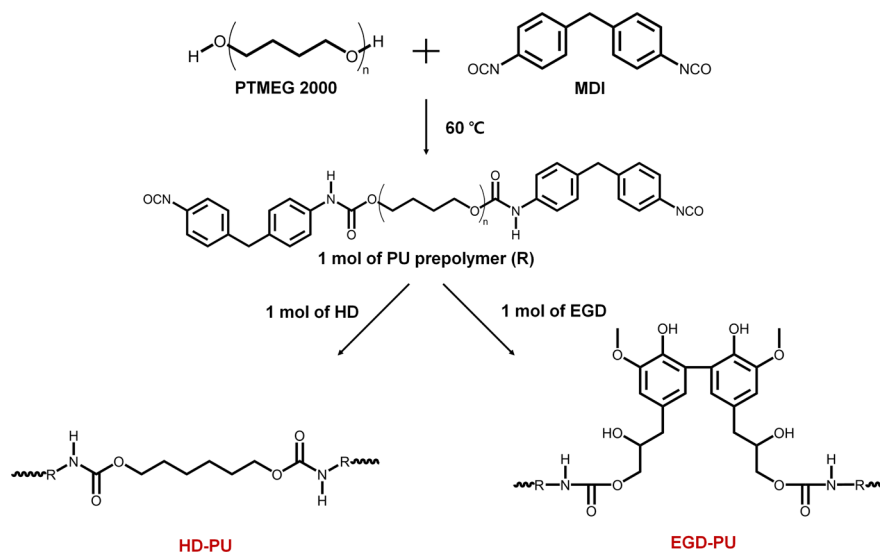


Figure 2. FTIR spectra of HD-PU and EGD-PU.

hinder oxidative dimerization by potassium ferricyanide. Herein, by protecting diol moiety, eugenol glycol was dimerized and EGD was successfully synthesized via deprotection. EGD was incorporated into the hard segment of PU with methylene diphenyl diisocyanate (MDI) to replace a traditional 1,6-hexanediol chain extender. Hence, EGD increased green carbon content in PU, and it is also expected to drive self-healing properties via reversible transcarbamoylation. In this study, eugenol glycol dimer-incorporated PU (EGD-PU) was characterized and examined in terms of its chemical compositions, thermal properties, physical properties, and self-healing properties.

## RESULTS AND DISCUSSIONS

**Synthesis of EGD.** A eugenol glycol dimer compound, EGD, was synthesized according to Scheme 1. First, eugenol glycol was obtained from eugenol through epoxidation by *m*-chloroperbenzoic acid (*m*CPBA) and further hydroxylation by sulfuric acid.<sup>42</sup> To dimerize eugenol glycol, the diol group in eugenol glycol was protected with the cyclic ketal group by the addition of *p*-toluenesulfonic acid (*p*-TSA) in acetone. Next, eugenol acetonide was oxidatively dimerized by  $K_3Fe_3(CN)_6$  between the C5 and C5' positions. The eugenol acetonide dimer was then deprotected by ether-HCl, and finally, EGD was obtained. The overall synthesis yield from eugenol glycol

to EGD was 40%. All the intermediate products in EGD synthesis were characterized by HPLC, GC-MS, and <sup>1</sup>H-NMR (Figures S1–S3). In the HPLC spectrum, the intermediates and the final product have retention times of 5.0 (eugenol glycol), 7.9 (eugenol acetonide), 15.1 (eugenol acetonide dimer), and 5.5 min (eugenol glycol dimer). The protection of the diol group and the further dimerization were shown to lead to a longer retention time in the C<sub>18</sub> column, which were attributed to increases in hydrophobicity and molecular weight, respectively. In GC-MS, the parent peaks of EGD intermediates with trimethylsilyl derivatization were observed, and their fragmentation pattern was also verified. The <sup>1</sup>H-NMR spectra of eugenol glycol showed peaks between 6.63 and 6.65 ppm; however, these peaks were not observed with EGD, indicating the formation of a covalent linkage between C5 and C5' of EGD (Figure 1).

**Synthesis of EGD-PU Film.** To synthesize EGD-PU, EGD was added as a chain extender during PU synthesis to initiate further polymerization with a prepolymer of poly(tetramethylene ether glycol) (PTMEG) and 4,4'-methylene diphenyl diisocyanate (MDI). The synthesis of EGD-PU was designed to form carbamate with two primary alcohols among six alcohols in EGD using the same molar ratio of the prepolymer (Scheme 2). EGD has two terminal primary alcohols that are much reactive than secondary and aromatic

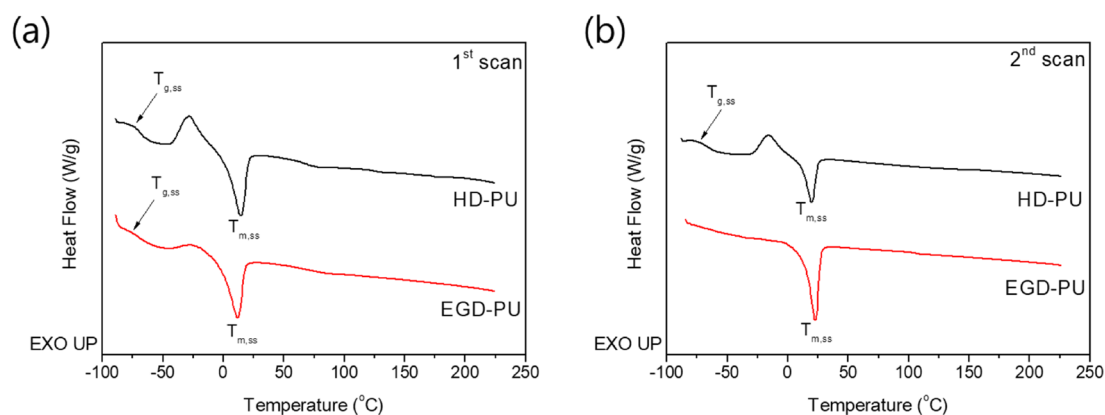


**Figure 3.** (a) First scan and (b) second scan of DSC thermograms of HD-PU and EGD-PU.  $T_{g,ss}$  denotes glass transition temperature of soft segments, and  $T_{m,ss}$  denotes melting transition temperature of soft segments.

alcohols. Therefore, EGD was expected to offer pendant hydroxyl groups to EGD-PU, which would then participate in the dynamic exchange reactions during the self-healing process. As a control, hexanediol polyurethane (HD-PU) was synthesized using 1,6-hexanediol, a conventional chain extender with a chain length similar to that of EGD.

The chemical structures of the obtained PU films were determined by FTIR analysis. The peak at  $2270\text{ cm}^{-1}$ , which corresponds to the NCO groups of the PU prepolymers, disappeared in the FTIR spectra of EGD-PU and HD-PU, indicating the successful incorporation of EGD and HD into PU as chain extenders, respectively. Urethane bonds were observed in all FTIR spectra at  $3297\text{ cm}^{-1}$  (N–H stretching),  $1733\text{ cm}^{-1}$  (urethane C=O),  $1538\text{ cm}^{-1}$  (N–H bending), and  $1602\text{ cm}^{-1}$  (aromatic ring) (Figure 2).<sup>44</sup> The profiles of the hydroxyl and carbonyl absorption bands showed remarkable differences between EGD-PU and HD-PU. In the FTIR spectrum of EGD-PU, the stretching vibrations of free O–H functional groups and C–O were clearly observed at  $3450$  and  $1262\text{ cm}^{-1}$ , respectively, and the additional peak of the aromatic ring derived from EGD was observed at  $1510\text{ cm}^{-1}$ . There was also a substantial difference in the aliphatic C–O stretching peak ranging from  $1090$  to  $1115\text{ cm}^{-1}$ . EGD-PU exhibited broad peaks of approximately  $1100\text{ cm}^{-1}$ , which were attributed to the C–O functional groups of the free hydroxyl group (C–O–H) in EGD (Figure 2), while both peaks attributed to C–O in PTMEG were observed in all FTIR spectra. These observations confirmed that EGD-PU has pendant hydroxyl groups in its molecular structure.

**Thermal Properties of PU Films.** The thermal properties of EGD-PU and HD-PU were evaluated using DSC measurement (Figure 3). The first heating thermograms of EGD-PU and HD-PU, which were prepared using different chain extenders, exhibited the general thermal behavior of a PU elastomer prepared using MDI and PTMEG 2000. The enthalpy change at  $-75\text{ °C}$  corresponds to the glass transition temperature ( $T_g$ ) of the soft segment of PUs, and EGD-PU and HD-PU had equal  $T_g$  values of  $-73.5$  and  $-74.2\text{ °C}$ , respectively.

The melting temperatures of PTMEG were observed to be  $12.1\text{ °C}$  for EGD-PU and  $15.0\text{ °C}$  for HD-PU, respectively. The second heating thermograms of the both PUs showed a slightly different trend than the first heating thermograms. HD-PU exhibited slightly higher  $T_g$  and  $T_m$  at  $-72.6$  and  $19.7\text{ °C}$ , respectively. By contrast, only the strong endothermic peak

corresponding to the melting of PTMEG was observed in EGD-PU at  $22.6\text{ °C}$  in the absence of  $T_g$ . This indicates that the amorphous phase of glass transition was not clearly observed as the crystallization of the soft segment of EGD-PU increased. HD-PU did not show a significant change in  $\Delta H_m$ , while EGD-PU showed a significant increase in  $\Delta H_m$  from  $19.1$  to  $36.0\text{ J/g}$ . (Table 1) Furthermore, thermogravimetric analysis (TGA) data showed decomposition temperatures of HD-PU and EGD-PU above  $300\text{ °C}$ . (Figure S5 and Table S1).

**Table 1. Thermal Properties of HD-PU and EGD-PU**

	HD-PU		EGD-PU	
	first heating	second heating	first heating	second heating
$T_g$ (°C)	-74.2	-72.6	-73.5	
$T_m$ (°C)	15.0	19.7	12.1	22.6
$\Delta H_m$ (J/g)	21.0	20.2	19.1	36.0

The stress–strain curves of EGD-PU and HD-PU in tensile tests are shown in Figure 4. EGD-PU ( $3.41\text{ MPa}$ ) exhibited a

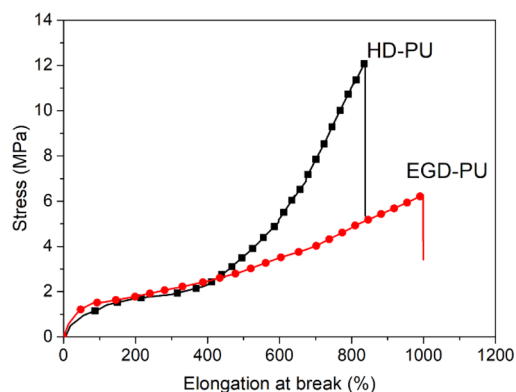


**Figure 4.** Stress–strain curves of HD-PU and EGD-PU.

slightly higher Young's modulus than HD-PU ( $2.69\text{ MPa}$ ), which is attributed to the introduction of the aromatic ring into the hard segment of EGD-PU additionally.<sup>46</sup> The tensile strength of EGD-PU ( $6.3\text{ MPa}$ ) was almost half that of HD-PU ( $12.1\text{ MPa}$ ) because the bulky aromatic structure and free hydroxyl groups in EGD weakens the physical cross-linking through the microphase separation of EGD-PU.<sup>45,46</sup> The packing of the hard segments is potentially interfered with the

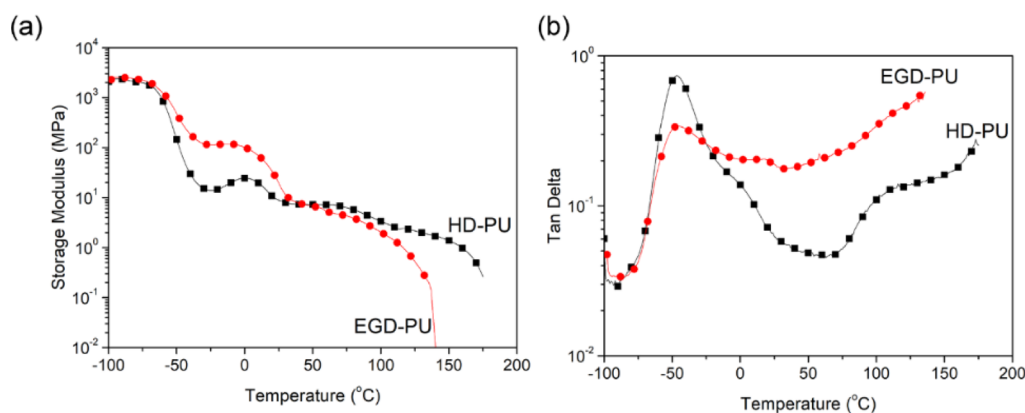


**Figure 5.** Dynamic mechanical properties of the HD-PU and EGD-PU: (a) storage modulus and (b) tan delta.

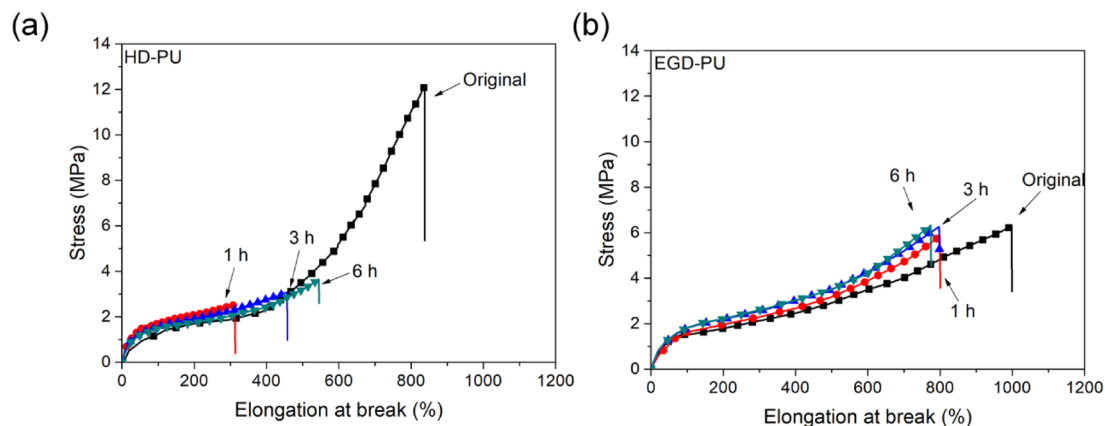


**Figure 6.** Self-healing property in tensile tests after heat treatments. (a) Stress–strain curves of pristine HD-PU and those after self-healing at 150 °C for 1, 3, and 6 h as well as (b) those for EGD-PU.

bulky groups, while C–O of PTMEG and the hard segment likely formed hydrogen bonds with the pendant hydroxyl groups. The strain hardening was hardly observed in the stress–strain curve of EGD-PU.

To confirm the presence of the microphase in the bulk morphology, SAXS analysis was conducted. In the plot of the scattering vector ( $q$ ) versus scattering intensity, both HD-PU and EGD-PU exhibited a single and broad peak.<sup>46</sup> This plotting indicates the presence of a phase-separated morphology in both HD-PU and EGD-PU. According to Bragg's law, the inter-domain distances of EGD-PU and HD-PU were 17 and 20 nm in SAXS, respectively (Figure S4). The shorter inter-domain distance of EGD-PU indicates less microphase separation between the hard segment and the soft segment in EGD-PU.

At temperatures under 20 °C, EGD-PU exhibited a higher storage modulus than HD-PU, since the introduction of EGD increased the contents of rigid aromatic rings. However, when the temperature increased up to the rubbery region, EGD-PU showed a lower storage modulus than HD-PU as well as a sharp decrease in modulus above 130 °C (Figure 5). This further decrease in modulus might be due to the exchanges between the urethane units and pendant hydroxyl groups of EGD.<sup>31,32,47</sup> A peak maximum was observed in the  $\tan \delta$  curves, for both  $T_g$  of EGD-PU and HD-PU,  $T_g$ s of  $-47.6$  and  $-46.9$  °C, respectively; these were comparable to the DSC measurement results. However, the  $\tan \delta$  curve of EGD-PU was found to be broader than that of HD-PU, indicating less

microphase separation of EGD-PU, as confirmed in SAXS (Figure 5).<sup>45</sup>

The thermal properties and glass transition temperature of EGD-PU were comparable to those of HD-PU in general. EGD-PU, chain-extended with bulky aromatic rings showed a higher Young's modulus and a lower tensile strength than HD-PU. The differences were attributed to lower microphase separation between the soft segment and hard segment in EGD-PU.

**Self-Healing Property of EGD-PU.** To evaluate the self-healing capacity of EGD-PU, the specimens were cut into halves, put together with gentle pressure at 150 °C for one of three time intervals (1, 3, and 6 h), and then pulled apart. EGD-PU showed excellent self-healing performance (99.84%) while HD-PU showed minimal self-healing ability (25.27%) in 3 h based on the molecular movement and diffusion above  $T_g$  (Figure 6, Table 2, and Figure S6). The self-healing efficiencies of the EGD-PU samples were all above 92.99%, and they were reinforced with increasing healing time.

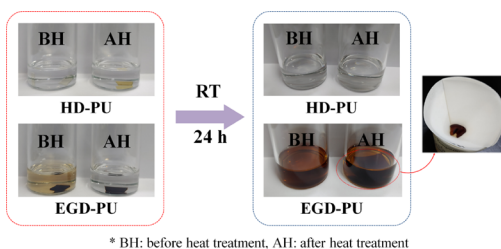
In addition, EGD-PU showed a high Young's modulus and tensile stress after self-healing, indicating that the dynamic carbamate exchange reactions enhanced the crack healing. It can be inferred that self-healing mainly comes from the exchange reaction between the free hydroxyl groups and the urethane group. To investigate the chemical structural change, the FTIR spectra of EGD-PU and HD-PU before and after self-healing at 150 °C are shown in Figure S7. FTIR spectrum of EGD-PU showed the decrease of peak intensity at 1120

**Table 2. Mechanical Properties of HD-PU and EGD-PU after Heat Treatment for 1, 3, and 6 h**

sample	healing time (h)	tensile stress (MPa)	elongation at break (%)	healing efficiency (%)
HD-PU	0	12.15	837.43	
	1	2.53	312.44	20.82
	3	3.07	456.19	25.27
	6	3.65	544.68	30.04
EGD-PU	0	6.28	998.19	
	1	5.84	799.26	92.99
	3	6.27	797.25	99.84
	6	6.32	774.06	100.64

$\text{cm}^{-1}$  corresponding to the secondary hydroxyl group after the self-healing process.<sup>48</sup> It indicates that the secondary alcohol groups in EGD-PU could be used in an exchange reaction with the carbamate groups at a specific temperature. On the other hand, these peaks of HD-PU were almost overlapped before and after the self-healing process because of the absence of the free hydroxyl groups in HD-PU. In addition, significant changes were found at 1710 (H-bonded carbonyl group) and 1735  $\text{cm}^{-1}$  (free carbonyl group) in the FTIR spectra (Figure S7e,f).<sup>49</sup> In the FTIR spectra of EGD-PU, the peak intensity of H-bonded urethane carbonyl group decreased after the self-healing at 150 °C compared with the sample before self-healing. While the HD-PU did not show the significant changes in the peak intensity of both the carbonyl groups before and after self-healing. It indicates that the hydrogen bond between the hard segments in EDG-PU was impeded by the structural changes or partial cross-linking due to the exchange reaction. That is, designed free hydroxyl in EGD-PU can efficiently contribute to the self-healing process of EGD-PU through the exchange reaction with carbamate groups. The exchange reaction with the nucleophilic addition of the free hydroxyl groups may cause a configuration change by forming cross-linking structures as well as a linear structure (Scheme S1).

To verify whether the exchange reaction changes the PU configuration, EGD-PU and HD-PU were immersed in DMF for 12 h to evaluate the gel fraction; they were then heat-treated. Both pristine PU films completely dissolved in DMF after 12 h. Heat-treated EGD-PU film swelled without any dissolution and obtained a gel fraction of 54.9%, whereas HD-PU dissolved completely after heat treatment for self-healing even though there were no changes in the chemical structure (Figure 7). The carbamate exchange reaction in EGD-PU not only rearranges molecular chains to repair damage but also



\* BH: before heat treatment, AH: after heat treatment

**Figure 7.** Gel fraction test results of the HD-PU and EGD-PU in dimethylformamide(DMF) before and after heat treatment. BH denotes samples before heat treatment and AH denotes those after heat treatment (photograph courtesy of Se-Ra Shin. Copyright 2021).

induces the partial gel-like structure, thereby enhancing the mechanical properties. The self-healing properties of EGD-PU and HD-PU were evaluated through three repeated cutting and healing tests (Figure 8); the results are summarized in Table 3. The results showed that the self-healing efficiency of HD-PU decreased significantly as the number of instance of cutting and healing increased. On the other hand, EGD-PU showed significantly higher self-healing performance in the three repeated tests. Although a slight decrease in tensile strength was observed in the third cutting and healing test, EGD-PU still exhibited a higher self-healing efficiency (84.7%) than HD-PU (11.87%). In addition, the crack in the EGD-PU sample healed without a scar (Figure S7). EGD-PU also showed great recyclability with a heat press at 130 °C for 5 min (Figure 9). EGD-PU is reprocessable with carbamate exchange after crack formation without a catalyst, and the cracks are removed under relatively mild conditions with high self-healing efficiency and repeatability.

**Antioxidant Effect of EGD-PU.** The antioxidant property is one of the most important factors for extending the lifespan of PU polymer while maintaining excellent physical properties.<sup>50,51</sup> It is expected that the aromatic hydroxyl groups in EGD could exhibit antioxidant properties due to their role as radical scavengers because they remained in the molecular chain without participating in the polymerization reaction. The antioxidant activity was evaluated using the DPPH method (Figure 10). EGD-PU exhibited 58.1% free radical scavenging activity after 30 min, whereas HD-PU showed little antioxidant activity (10.9%). The DPPH solution containing EGD-PU changed its color from purple to dark yellow, indicating that the aromatic hydroxyl groups in EGD-PU impart excellent antioxidant activity to PU by stabilizing the free radical. The antioxidant properties of this self-healing PU are expected to provide a longer life span and resistance to oxidative degradation of PU films. Oxidation of PU makes aging faster and the mechanical strength of PU weaker. Therefore, some researchers added antioxidants such as vitamin E during PU synthesis.<sup>52</sup> EGD-PU has an antioxidant effect itself derived from EGD containing phenol group expecting a longer life span.

## CONCLUSIONS

We developed a bio-based self-healing PU with antioxidant properties by introducing a novel polyol chain extender EGD. To produce a symmetrical chain extender from eugenol glycol, we used a protection-coupling-deprotection system. After protecting the vicinal diol, a yield of 40% was obtained in a day without the production of any byproducts. Notably, the chemical EGD has never been reported and synthesized from eugenol. The prepared EGD-PU showed a high self-healing efficiency and repetitive self-healing property through transcarbamoylation by pendant hydroxyl groups at 150 °C. EGD-PU may have the potential to apply for self-healing coating or adhesives. Repetitive self-healing with high efficiency is expected to have great applicability compared with urethane bond exchange using only a phenolic compound or a Diels–Alder reaction.<sup>53,54</sup>

In addition, EGD was obtained from eugenol oxide dimer by hydroxylation. Interestingly, eugenol oxide was successfully dimerized with high yield by laccase from *Trametes versicolor* (Scheme S2). The synthesis of EGD through the enzymatic reaction can be advantageous because of the short chemical steps involved, and this will be further studied by our group.

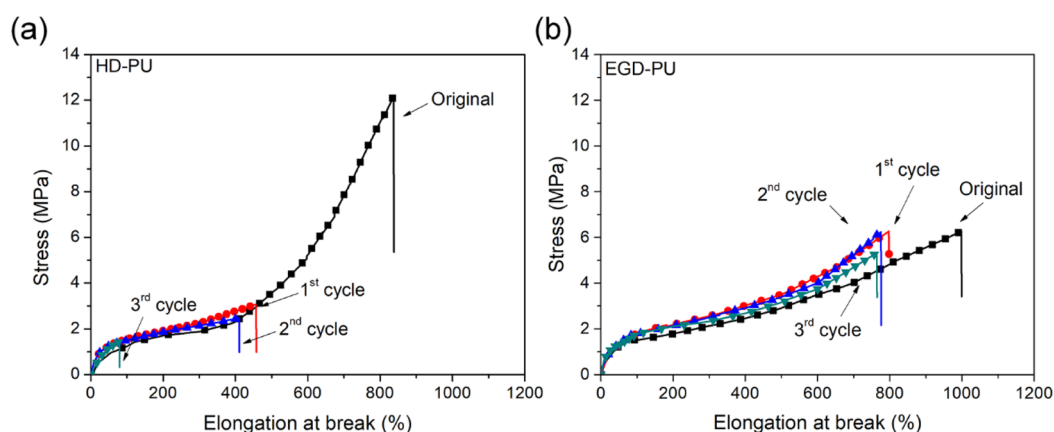


**Figure 8.** Tensile properties of recycled polyurethane elastomer sheets after repeated crushing and hot press remolding: (a) HD-PU; (b) EGD-PU.

**Table 3. Mechanical Properties of HD-PU and EGD-PU after Three Times Repeated Self-Healing Tests**

sample	number of cycles	tensile stress (MPa)	elongation at break (%)	healing efficiency (%)
HD-PU	original	12.15	837.43	
	first	3.07	456.19	25.27
	second	2.47	410.00	20.33
	third	1.44	79.26	11.85
EGD-PU	original	6.28	998.19	
	first	6.27	797.25	99.84
	second	6.24	775.73	99.36
	third	5.32	764.05	84.71

In addition, eugenol, as a lignin decomposition byproduct, was upcycled into bio-based self-healing PUs. In particular, the alkene group in eugenol can be modified into a diol group. This study showed that the pairs of different hydroxyl groups by dimerization are important in imparting different effects on PU such as the self-healing and antioxidant properties. The effect of hydroxyl group number or position variations on the dynamic properties of PUs needs to be further analyzed utilizing other lignin-degraded aromatic monomers.

## EXPERIMENTAL SECTION

**Materials.** Eugenol (Sigma, 99%), *m*CPBA (Acros organics, 77%), sodium sulfite (Junsei), sodium sulfate (Tedea) H<sub>2</sub>SO<sub>4</sub> (Duksan), sodium bicarbonate (Duksan), 4,4'-methylene diphenyl diisocyanate (MDI), poly(tetramethylene ether glycol) (PTMEG) (number average molecular weight ( $M_n$ ) = 2000 g/mol), and 1,6-hexanediol (HD) were all purchased from Sigma Aldrich (Yong-in, Korea). All chemicals were of analytical grade and used as received except for PTMEG and HD, which were both vacuum dried at 70 °C for 24 h before use. *N,N*-dimethylformamide (DMF) was used as a solvent in the preparation of PU. The reactions were analyzed by thin layer chromatography (TLC) using pre-coated silica gel plates (TLC Silica gel 60 F254, 250 μm thickness from Merck). Flash column chromatography was conducted on silica gel 60 (particle size 0.04–0.063 mm from Merck or Sigma-Aldrich).

**NMR, HPLC, and GC Analysis.** Nuclear magnetic resonance (NMR) spectra were recorded on a Bruker Avance III 400 FT-NMR spectrometer using residual solvent peaks as



**Figure 9.** Recyclable capacity of EGD-PU with a hot press (photograph courtesy of Se-Ra Shin. Copyright 2021).

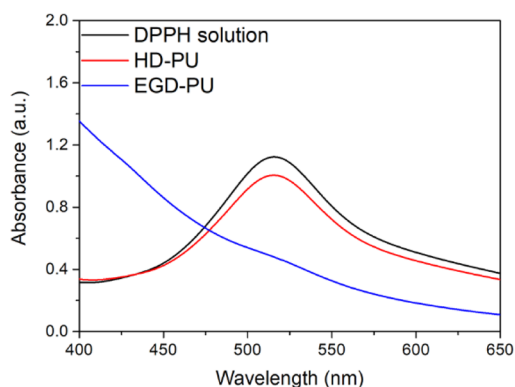


**Figure 10.** Antioxidant effect of EGD-PU in DPPH (photograph courtesy of Se-Ra Shin. Copyright 2021).

an internal standard (DMSO- $d_6$  @ 2.50 ppm  $^1\text{H}$  NMR). The following abbreviations (or combinations thereof) were used to explain the multiplicities: *s* = singlet, *d* = doublet, *t* = triplet, *q* = quartet, *m* = multiplet. High-pressure liquid chromatography (HPLC) spectra were collected on YoungLin equipped with a Waters  $\mu$ Bondapak C18 column (3.9  $\times$  300 mm). Eugenol derivatives were detected with UV at 280 nm. The mobile phase was composed of 10% acetonitrile (ACN) and 90% water containing 0.1% trifluoroacetic acid (TFA) with a flow rate of 0.7 mL/min. The concentration of ACN was increased to 50% for 20 min and then decreased to 10% for 5 min, before finally being held there for 5 min. Gas chromatography mass spectrometry (GC–MS) spectra were collected on ITQ1100. Products were derivatized with *N,O*-bis-(trimethylsilyl)-trifluoroacetamide (BSTFA) at 50  $^\circ\text{C}$  for 10 min, and they were analyzed with GC–MS using the electron impact (EI) ionization method. The initial temperature was 50  $^\circ\text{C}$  for 3 min, and this was increased at a 3  $^\circ\text{C}/\text{min}$  rate until 270  $^\circ\text{C}$ , before being held at the highest temperature for 10 min.

**Synthesis of Eugenol Oxide (2-Methoxy-4-(2-oxiranylmethyl)phenol).** Eugenol (5.3 g, 32 mmol) was dissolved in dichloromethane (100 mL), and then a solution of *m*-CPBA (11.15 g, 55 mmol) in dichloromethane (100 mL) was added dropwise. Next, the solution was poured into an excess of ice-water for 30 min and stirred at room temperature for 12 h. At this point, the reaction mixture was poured into an excess of ice-water, then the precipitated *m*-CBA was filtered by a vacuum filter using a 0.45  $\mu\text{m}$  membrane filter. To neutralize the oxidizing agent, the resulting mixture was worked up with 200 mL of 10% aqueous sodium sulfite. The organic phase was washed twice with aqueous sodium bicarbonate and then once with brine, before finally being dried on anhydrous sodium sulfate. After filtration, the filtrate was condensed to remove the solvent, and the residue was further purified on a silica gel column (hexane/ethyl acetate = 20:1, v/v) to obtain the epoxide intermediate as a light yellow oil [3.2 g; 55%].  $^1\text{H}$  NMR (400 MHz, DMSO- $d_6$ , TMS):  $\delta$  (ppm) 8.74 (*s*, 1H), 6.82 (*d*, *J* = 1.8 Hz, 1H), 6.71 (*d*, *J* = 6.0 Hz, 1H), 6.65–6.63 (*m*, 1H), 3.75 (*s*, 3H), 3.07–3.05 (*m*, 1H), 2.73–2.62 (*m*, 3H), 2.54–2.52 (*m*, 1H); GC–MS (EI, 70 eV): *m/z* 252.45 (40%,  $\text{M}^+$ -TMS), 237.40 (50), 222.35 (100), 179.32 (60), 73.10 (20).

**Synthesis of Eugenol Glycol (3-(4-Hydroxy-3-methoxyphenyl)propane-1,2-diol).** Eugenol oxide (40 g, 222 mmol) was dissolved in dichloromethane (DCM) (400 mL) and treated with 400 mL of distilled water and 200 mL of 5%  $\text{H}_2\text{SO}_4$  solution. The solution was stirred at room temperature for 24 h, after which DCM was removed by evaporation. The aqueous solution was extracted three times with EA and twice with DE and then dried on anhydrous sodium sulfate. After filtration, the filtrate was condensed to remove the solvent, and the residue was further purified on a silica gel column (dichloromethane/methanol = 20:1, v/v) to obtain the glycol intermediate as a yellowish orange oil [31 g, 67%].  $^1\text{H}$  NMR (400 MHz, DMSO- $d_6$ , TMS):  $\delta$  (ppm) 8.61 (*s*, 1H), 6.76 (*d*, *J* = 1.61 Hz, 1H), 6.65 (*d*, *J* = 7.95 Hz, 1H), 6.59–6.56 (*m*, 1H), 4.49–4.44 (*m*, 2H), 3.73 (*s*, 3H), 3.57–3.54 (*m*, 1H), 3.27–3.24 (*m*, 2H), 2.65–2.39 (*m*, 2H); GC–MS (EI, 70 eV): *m/z* 414.98 (6%,  $\text{M}^+$ -TMS), 342.84 (30), 324.86 (100), 293.81 (20), 209.60 (45), 89.27 (10).

**Synthesis of Eugenol Acetonide (4-((2,2-Dimethyl-1,3-dioxolan-4-yl)methyl)-2-methoxyphenol).** Eugenol

glycol (30 g, 151 mmol) was dissolved in a mixture of acetone (450 mL) and 5 mol % *p*TSA; anhydrous  $\text{MgSO}_4$  (50 mg) was also added to remove any residual water. The mixture was stirred at room temperature until complete conversion and then analyzed by thin layer chromatography. The resulting mixture was passed through a silica gel to remove the remaining *p*TSA and  $\text{MgSO}_4$ . After filtration, the filtrate was evaporated under reduced pressure, and acetonide intermediate was obtained as a light yellowish brown oil [35 g, 98%].  $^1\text{H}$  NMR (400 MHz, DMSO- $d_6$ ):  $\delta$  (ppm) 8.70 (*s*, 1H), 6.80 (*d*, *J* = 1.82 Hz, 1H), 6.68 (*d*, *J* = 7.91 Hz, 1H), 6.62–6.59 (*m*, 1H), 4.25–4.19 (*m*, 1H), 3.89–3.86 (*m*, 1H), 3.74 (*s*, 3H), 3.55–3.51 (*m*, 1H), 2.79–2.61 (*m*, 2H), 1.32 (*s*, 3H), 1.25 (*s*, 3H); GC–MS (EI, 70 eV): 310.67 (100%,  $\text{M}^+$ -TMS), 295.65 (40), 235.60 (42), 209.51 (95), 195.47 (37), 179.45 (80), 101.28 (95).

**Synthesis of Eugenol Acetonide Dimer (5,5'-Bis((2,2-dimethyl-1,3-dioxolan-4-yl)methyl)-3,3'-dimethoxy-[1,1'-bisphenyl]-2,2'-diol).** Eugenol acetonide (35 g, 147 mmol) was first dissolved in acetone (450 mL) and distilled water (225 mL), then 25%  $\text{NH}_4\text{OH}$  (300 mL) was added, and the mixture was stirred for 10 min. Next, a saturated aqueous solution of  $\text{K}_3\text{Fe}(\text{CN})_6$  (47 g, 154 mmol, 1.05 eq.) was added dropwise to the solution over 3 h. Later, more  $\text{NH}_4\text{OH}$  (300 mL) was added to maintain the alkalinity in the reaction solution, and the mixture was stirred overnight at room temperature. After TLC indicated the complete consumption of the reactants, the volatile component was removed through evaporation. The aqueous solution was extracted three times with EA and twice with DE and then dried on anhydrous sodium sulfate. After filtration, the filtrate was condensed to remove the solvent. The residue was further purified on a silica gel column (hexane/acetone = 3:2, v/v) to obtain the acetonide dimer as a brownish yellow oil [16 g, 47%].  $^1\text{H}$  NMR (400 MHz, DMSO- $d_6$ ):  $\delta$  (ppm) 8.25 (*s*, 2H), 6.80 (*d*, *J* = 1.94 Hz, 2H), 6.60 (*d*, *J* = 1.97 Hz, 2H), 4.30–4.22 (*m*, 2H), 3.93–3.89 (*m*, 2H), 3.80 (*s*, 6H), 3.59–3.55 (*m*, 2H), 2.82–2.64 (*m*, 4H), 1.33 (*s*, 6H), 1.25 (*s*, 6H); GC–MS (EI, 70 eV): *m/z* 618.95 (70%,  $\text{M}^+$ -TMS), 517.86 (100), 207.34 (50), 101.21 (10).

**Synthesis of Eugenol Glycol Dimer (3,3'-(6,6'-Dihydroxy-5,5'-dimethoxy-[1,1'-biphenyl]-3,3'-diyl)bis(propene-1,2-diol).** Eugenol acetonide dimer (16 g, 34 mmol) was dissolved in ether-HCl (300 mL) and water (40 mL), and then the mixture was stirred for 3 h. After TLC indicated the complete consumption of the reactants, the reaction mixture was condensed to remove the solvent. Next, the residue was freeze-dried overnight to obtain the eugenol glycol dimer product as a brownish oil [12 g, 87%].  $^1\text{H}$  NMR (400 MHz, DMSO- $d_6$ ):  $\delta$  (ppm) 8.16 (*s*, 2H), 6.79 (*d*, *J* = 1.87 Hz, 2H), 6.58 (*d*, *J* = 1.83 Hz, 2H), 4.51 (*s*, 4H), 3.80 (*s*, 6H), 3.61 (*s*, 2H), 3.30 (*s*, 4H), 2.70–2.43 (*m*, 4H); GC–MS (EI, 70 eV): *m/z* 827.01 (40%,  $\text{M}^+$ -TMS), 736.96 (35), 646.89 (40), 89.16 (15).

**Synthesis of PU Films.** Two types of PU films with different chain extenders (HD and EGD) were prepared using the prepolymer method. First, PTMEG (1 mol) and MDI (2 mol) were weighted into a four-neck round-bottom flask, and the temperature was increased to 50  $^\circ\text{C}$  to obtain a homogeneous mixture. The reaction was conducted at 60  $^\circ\text{C}$  under a nitrogen atmosphere until the NCO% reached the theoretical value. The NCO% value was determined by the back-titration method followed by ASTM D 1638-74. Next,

the PU prepolymer was dissolved in DMF and the stoichiometric amount of chain extender (1 mol of HD or EGD) was added to the PU prepolymer. In this work, EGD was regarded as a diol despite having the six free hydroxyl groups. Thus, it was expected that four hydroxyl groups might take part in the exchange reactions with urethane units. After 3 h, the solution was poured into a Teflon mold, which was then placed in a convection oven set at 110 °C for 1 day to remove the solvent. The PU films, which were prepared using HD and EGD as chain extenders, were named HD-PU and EGD-PU, respectively. Scheme 2 shows the scheme used for the preparation of PU films.

**Characterization of PU Films.** Fourier transform infrared (FTIR) was used to confirm the chemical structure of HD-PU and EGD-PU through FTIR spectroscopy (FTIR 4600, JASCO). The FTIR spectra of PU films were obtained using an attenuated total reflectance (ATR) accessory at a resolution of 4 cm<sup>-1</sup> at room temperature. The thermal analyses of both PUs were carried out using differential scanning calorimetry (DSC) (Q20, TA instrument). About 5 mg of the sample was sealed in a platinum pan then measured at a heating rate of 10 °C/min with a nitrogen atmosphere. The dynamic mechanical properties of HD-PU and EGD-PU were investigated using a dynamic mechanical analyzer (DMA) (Q800, TA instrument). The thermal stability was characterized from 40–800 °C, employing a thermogravimetric analyzer (TGA) (Q600, TA) at a heating rate of 20 °C/min in a N<sub>2</sub> environment. A sample with the dimensions of 15 mm × 5.3 mm × 0.7 mm (length × width × thickness) was studied in the range from –100 to 200 °C at a heating rate of 5 °C/min. The tensile properties and self-healing efficiency of PU films were investigated using a universal testing machine (UTM) (LR5K Plus, LLOYD); the crosshead speed was controlled at 500 mm/min. The four specimens with a dog-bone shape were measured and averaged to obtain the representative data. Small-angle X-ray scattering patterns of PU films were obtained with a Xenocs XEUS2.0 within the scattering range from  $q \approx 0.00035$  to 0.176 Å<sup>-1</sup>. The self-healing efficiency was calculated using the following equation.

$$\text{self-healing efficiency(\%)} = \sigma_{\text{healed}} / \sigma_{\text{original}} \times 100$$

where  $\sigma_{\text{original}}$  corresponds to the sample tensile strength before self-healing and  $\sigma_{\text{healed}}$  corresponds to the sample tensile strength after self-healing at 150 °C.

**Antioxidant Activity of PU Films.** The antioxidant activity of PU samples was evaluated according to the 2,2-diphenyl-1-picrylhydrazyl (DPPH) method.<sup>41,55,56</sup> Each PU sample (100 mg) was immersed in 0.3 mM DPPH methanol solution in the dark. After 30 min, the absorbance of the DPPH solution was measured by employing UV–Vis spectrometer (JASCO V-670, Easton, MD, USA) at  $\lambda = 515$  nm. The antioxidant activity (%) was calculated as follows:

$$\text{antioxidant activity (\%)} = \left[ \frac{A_b - A_s}{A_b} \right] \times 100$$

where  $A_b$  and  $A_s$  are the absorbance of DPPH solution without PU sample and with PU sample (EDH-PU or HD-PU), respectively.

## ■ ASSOCIATED CONTENT

### Supporting Information

The Supporting Information is available free of charge at <https://pubs.acs.org/doi/10.1021/acsomega.1c03802>.

Chemical analysis of eugenol glycol dimer and intermediates by HPLC (Figure S1), GC–MS (Figure S2), and <sup>1</sup>H-NMR (Figure S3); PU sample analysis with small-angle X-ray scattering (SAXS) analysis (Figure S4) and thermogravimetric analysis (TGA) (Figure S5 and Table S1); dog-bone shaped PU samples after self-healing process (Figure S6); chemical structural change after self-healing (Figure S7); possible self-healing network (Scheme S1); and chemical reaction scheme of EGD synthesis (Scheme S2) (PDF)

## ■ AUTHOR INFORMATION

### Corresponding Authors

**Dai-Soo Lee** – Research Institute, Jungwoo Fine Co., Ltd., Iksan, Jeollabuk-do 54586, Republic of Korea; Email: [dslee@jbnu.ac.kr](mailto:dslee@jbnu.ac.kr)

**Byung-Gee Kim** – School of Chemical and Biological Engineering, Seoul National University, 08826 Seoul, Republic of Korea; Institute of Molecular Biology and Genetics, Seoul National University, Seoul 08826, Republic of Korea; Institute of Bioengineering in Bio-Max, Seoul National University, Seoul 08826, Republic of Korea; Institute for Sustainable Development (ISD), Seoul National University, Seoul 08826, South Korea; [orcid.org/0000-0002-3776-1001](https://orcid.org/0000-0002-3776-1001); Phone: +82-2-880-8945; Email: [byungkim@snu.ac.kr](mailto:byungkim@snu.ac.kr); Fax: +82-2-876-8945

### Authors

**Uk-Jae Lee** – School of Chemical and Biological Engineering, Seoul National University, 08826 Seoul, Republic of Korea; Institute of Molecular Biology and Genetics, Seoul National University, Seoul 08826, Republic of Korea

**Se-Ra Shin** – Research Institute, Jungwoo Fine Co., Ltd., Iksan, Jeollabuk-do 54586, Republic of Korea

**Heewon Noh** – School of Chemical and Biological Engineering, Seoul National University, 08826 Seoul, Republic of Korea; Institute of Molecular Biology and Genetics, Seoul National University, Seoul 08826, Republic of Korea

**Han-Bit Song** – School of Chemical and Biological Engineering, Seoul National University, 08826 Seoul, Republic of Korea; Institute of Molecular Biology and Genetics, Seoul National University, Seoul 08826, Republic of Korea

**Junyeob Kim** – School of Chemical and Biological Engineering, Seoul National University, 08826 Seoul, Republic of Korea; Institute of Molecular Biology and Genetics, Seoul National University, Seoul 08826, Republic of Korea

Complete contact information is available at:

<https://pubs.acs.org/doi/10.1021/acsomega.1c03802>

### Author Contributions

#U.J.L., S.R.S., and H.W.N. contributed equally to this work. B.G.K., D.S.L., U.J.L., and H.W.N. designed experiments. B.G.K., D.S.L., U.J.L., S.R.S., and H.W.N. prepared the paper. U.J.L. and H.W.N. synthesized and characterized EGD. H.B.S. and J.Y.K. purified EGD. S.R.S., D.S.L. synthesized EGD-PU

and characterized EGD-PU. The manuscript was written through contributions of all authors. All authors have given approval to the final version of the manuscript.

## Notes

The authors declare no competing financial interest.

## ACKNOWLEDGMENTS

This work was supported by Industrial Strategic technology development program, 10049677, funded by the Ministry of Trade, Industry & Energy (MI, Korea) and the Korea Medical Device Development Fund grant funded by the Korean government (the Ministry of Science and ICT, the Ministry of Trade, Industry and Energy, the Ministry of Health & Welfare, the Ministry of Food and Drug Safety) (project number: KMDF\_PR\_20200901\_0151).

## ABBREVIATIONS

PU, polyurethane; EGD, eugenol glycol dimer; MDI, 4,4'-methylene diphenyl diisocyanate; DSC, differential scanning calorimeter; DMA, dynamic mechanical analyzer; UTM, universal testing machine; HPLC, high-pressure liquid chromatography; NMR, nuclear magnetic resonance

## REFERENCES

- (1) Gang, H.; Lee, D.; Choi, K.-Y.; Kim, H.-N.; Ryu, H.; Lee, D.-S.; Kim, B.-G. Development of high performance polyurethane elastomers using vanillin-based green polyol chain extender originating from lignocellulosic biomass. *ACS Sustainable Chem. Eng.* **2017**, *5*, 4582–4588.
- (2) Laurichesse, S.; Huillet, C.; Avérous, L. Original polyols based on organosolv lignin and fatty acids: new bio-based building blocks for segmented polyurethane synthesis. *Green Chem.* **2014**, *16*, 3958–3970.
- (3) Xing, W.; Yuan, H.; Zhang, P.; Yang, H.; Song, L.; Hu, Y. Functionalized lignin for halogen-free flame retardant rigid polyurethane foam: preparation, thermal stability, fire performance and mechanical properties. *J. Polym. Res.* **2013**, *20*, 234.
- (4) Kai, D.; Zhang, K.; Jiang, L.; Wong, H. Z.; Li, Z.; Zhang, Z.; Loh, X. J. Sustainable and antioxidant lignin–polyester copolymers and nanofibers for potential healthcare applications. *ACS Sustainable Chem. Eng.* **2017**, *5*, 6016–6025.
- (5) Saito, T.; Brown, R. H.; Hunt, M. A.; Pickel, D. L.; Pickel, J. M.; Messman, J. M.; Baker, F. S.; Keller, M.; Naskar, A. K. Turning renewable resources into value-added polymer: development of lignin-based thermoplastic. *Green Chem.* **2012**, *14*, 3295–3303.
- (6) Akindoyo, J. O.; Beg, M. D. H.; Ghazali, S.; Islam, M. R.; Jeyaratnam, N.; Yuvaraj, A. R. Polyurethane types, synthesis and applications—a review. *RSC Adv.* **2016**, *6*, 114453–114482.
- (7) Bayer, O.; Siefken, W.; Rinke, H.; Orthner, L.; Schild, H. A process for the production of polyurethanes and polyureas. *German Patent DRP 11/13/1937*, 728,981, 1937.
- (8) Nohra, B.; Candy, L.; Blanco, J.-F.; Guerin, C.; Raoul, Y.; Mouloungui, Z. From petrochemical polyurethanes to biobased polyhydroxyurethanes. *Macromolecules* **2013**, *46*, 3771–3792.
- (9) Upton, B. M.; Kasko, A. M. Strategies for the conversion of lignin to high-value polymeric materials: review and perspective. *Chem. Rev.* **2016**, *116*, 2275–2306.
- (10) Javni, I.; Zhang, W.; Petrović, Z. S. Effect of different isocyanates on the properties of soy-based polyurethanes. *J. Appl. Polym. Sci.* **2003**, *88*, 2912–2916.
- (11) Xue, B.-L.; Wen, J.-L.; Sun, R.-C. Lignin-based rigid polyurethane foam reinforced with pulp fiber: synthesis and characterization. *ACS Sustainable Chem. Eng.* **2014**, *2*, 1474–1480.
- (12) Zhang, C.; Ding, R.; Kessler, M. R. Reduction of epoxidized vegetable oils: a novel method to prepare bio-based polyols for polyurethanes. *Macromol. Rapid Commun.* **2014**, *35*, 1068–1074.
- (13) Ciobanu, C.; Ungureanu, M.; Ignat, L.; Ungureanu, D.; Popa, V. I. Properties of lignin–polyurethane films prepared by casting method. *Ind. Crops Prod.* **2004**, *20*, 231–241.
- (14) Chung, H.; Washburn, N. R. Improved lignin polyurethane properties with lewis acid treatment. *ACS Appl. Mater. Interfaces* **2012**, *4*, 2840–2846.
- (15) Liang, J.-Y.; Shin, S.-R.; Lee, S.-H.; Lee, D.-S. Characteristics of Self-Healable Copolymers of Styrene and Eugenol Terminated Polyurethane Prepolymer. *Polymer* **2019**, *11*, 1674.
- (16) Rowan, S. J.; Cantrill, S. J.; Cousins, G. R. L.; Sanders, J. K. M.; Stoddart, J. F. Dynamic covalent chemistry. *Angew. Chem., Int. Ed.* **2002**, *41*, 898–952.
- (17) Skene, W. G.; Lehn, J.-M. P. Dynamers: polyacylhydrazone reversible covalent polymers, component exchange, and constitutional diversity. *Proc. Natl. Acad. Sci. U. S. A.* **2004**, *101*, 8270–8275.
- (18) Dahlke, J.; Zechel, S.; Hager, M. D.; Schubert, U. S. How to design a self-healing polymer: general concepts of dynamic covalent bonds and their application for intrinsic healable materials. *Adv. Mater. Interfaces* **2018**, *5*, 1800051.
- (19) Guimard, N. K.; Oehlenschlaeger, K. K.; Zhou, J.; Hilf, S.; Schmidt, F. G.; Barner-Kowollik, C. Current trends in the field of self-healing materials. *Macromol. Chem. Phys.* **2012**, *213*, 131–143.
- (20) Huynh, T. P.; Sonar, P.; Haick, H. Advanced materials for use in soft self-healing devices. *Adv. Mater.* **2017**, *29*, 1604973.
- (21) Lutz, A.; van den Berg, O.; Van Damme, J.; Verheyen, K.; Bauters, E.; De Graeve, I.; Du Prez, F. E.; Terryn, H. A shape-recovery polymer coating for the corrosion protection of metallic surfaces. *ACS Appl. Mater. Interfaces* **2015**, *7*, 175–183.
- (22) Kessler, M. R. Self-healing: a new paradigm in materials design. *Proc. Inst. Mech. Eng., Part G* **2007**, *221*, 479–495.
- (23) Zhou, J.; Liu, H.; Sun, Y.; Wang, C.; Chen, K. Self-Healing Titanium Dioxide Nanocapsules-Graphene/Multi-Branched Polyurethane Hybrid Flexible Film with Multifunctional Properties toward Wearable Electronics. *Adv. Funct. Mater.* **2021**, *31*, 2011133.
- (24) Li, X.; Yu, R.; He, Y.; Zhang, Y.; Yang, X.; Zhao, X.; Huang, W. Self-Healing Polyurethane Elastomers Based on a Disulfide Bond by Digital Light Processing 3D Printing. *ACS Macro Lett.* **2019**, *8*, 1511–1516.
- (25) Chao, A.; Negulescu, I.; Zhang, D. Dynamic covalent polymer networks based on degenerative imine bond exchange: tuning the malleability and self-healing properties by solvent. *Macromolecules* **2016**, *49*, 6277–6284.
- (26) Cromwell, O. R.; Chung, J.; Guan, Z. Malleable and self-healing covalent polymer networks through tunable dynamic boronic ester bonds. *J. Am. Chem. Soc.* **2015**, *137*, 6492–6495.
- (27) Canadell, J.; Goossens, H.; Klumperman, B. Self-healing materials based on disulfide links. *Macromolecules* **2011**, *44*, 2536–2541.
- (28) Sridhar, L. M.; Oster, M. O.; Herr, D. E.; Gregg, J. B. D.; Wilson, J. A.; Slark, A. T. Re-usable thermally reversible crosslinked adhesives from robust polyester and poly (ester urethane) Diels–Alder networks. *Green Chem.* **2020**, *22*, 8669–8679.
- (29) Ying, H.; Zhang, Y.; Cheng, J. Dynamic urea bond for the design of reversible and self-healing polymers. *Nat. Commun.* **2014**, *5*, 3218.
- (30) Zheng, N.; Fang, Z.; Zou, W.; Zhao, Q.; Xie, T. Thermoset shape-memory polyurethane with intrinsic plasticity enabled by transcarbamoylation. *Angew. Chem.* **2016**, *128*, 11593–11597.
- (31) Fortman, D. J.; Brutman, J. P.; Cramer, C. J.; Hillmyer, M. A.; Dichtel, W. R. Mechanically activated, catalyst-free polyhydroxyurethane vitrimers. *J. Am. Chem. Soc.* **2015**, *137*, 14019–14022.
- (32) Fortman, D. J.; Brutman, J. P.; Hillmyer, M. A.; Dichtel, W. R. Structural effects on the reprocessability and stress relaxation of crosslinked polyhydroxyurethanes. *J. Appl. Polym. Sci.* **2017**, *134*, 44984.
- (33) Liu, W.; Fang, C.; Wang, S.; Huang, J.; Qiu, X. High-performance lignin-containing polyurethane elastomers with dynamic covalent polymer networks. *Macromolecules* **2019**, *52*, 6474–6484.

- (34) Kamatou, G. P.; Vermaak, I.; Viljoen, A. M. Eugenol—from the remote Maluku Islands to the international market place: a review of a remarkable and versatile molecule. *Molecules* **2012**, *17*, 6953–6981.
- (35) Sakai, K.; Takeuti, H.; Mun, S.-P.; Imamura, H. Formation of isoeugenol and eugenol during the cleavage of  $\beta$ -aryl ethers in lignin by alcohol-bisulfite treatment. *J. Wood Chem. Technol.* **1988**, *8*, 29–41.
- (36) Faye, I.; Decostanzi, M.; Ecochard, Y.; Caillol, S. Eugenol bio-based epoxy thermosets: from cloves to applied materials. *Green Chem.* **2017**, *19*, S236–S242.
- (37) Cheng, C.; Li, J.; Yang, F.; Li, Y.; Hu, Z.; Wang, J. Renewable eugenol-based functional polymers with self-healing and high temperature resistance properties. *J. Polym. Res.* **2018**, *25*, 57.
- (38) Liu, K.; Madbouly, S. A.; Kessler, M. R. Biorenewable thermosetting copolymer based on soybean oil and eugenol. *Eur. Polym. J.* **2015**, *69*, 16–28.
- (39) Bortolomeazzi, R.; Verardo, G.; Liessi, A.; Callea, A. Formation of dehydrodiisoeugenol and dehydrodieugenol from the reaction of isoeugenol and eugenol with DPPH radical and their role in the radical scavenging activity. *Food Chem.* **2010**, *118*, 256–265.
- (40) Gülçin, I. Antioxidant activity of eugenol: A structure–activity relationship study. *J. Med. Food* **2011**, *14*, 975–985.
- (41) Modjinou, T.; Versace, D.-L.; Abbad-Andaloussi, S.; Langlois, V.; Renard, E. Antibacterial and antioxidant photoinitiated epoxy co-networks of resorcinol and eugenol derivatives. *Mater. Today Commun.* **2017**, *12*, 19–28.
- (42) Dalko, M.; Hitce, J. 1-phenylmono-or-polyhydroxypropane compounds, compositions and cosmetic uses thereof. U.S. Patent US10,307,353B2 **06/04/2019**.
- (43) de Farias Dias, A. An improved high yield synthesis of dehydrodieugenol. *Phytochemistry* **1988**, *27*, 3008–3009.
- (44) Nozaki, S.; Hirai, T.; Higaki, Y.; Yoshinaga, K.; Kojio, K.; Takahara, A. Effect of chain architecture of polyol with secondary hydroxyl group on aggregation structure and mechanical properties of polyurethane elastomer. *Polymer* **2017**, *116*, 423–428.
- (45) Caracciolo, P. C.; Buffa, F.; Abraham, G. A. Effect of the hard segment chemistry and structure on the thermal and mechanical properties of novel biomedical segmented poly (esterurethanes). *J. Mater. Sci.: Mater. Med.* **2009**, *20*, 145–155.
- (46) Behera, P. K.; Mondal, P.; Singha, N. K. Polyurethane with an ionic liquid crosslinker: a new class of super shape memory-like polymers. *Polym. Chem.* **2018**, *9*, 4205–4217.
- (47) Chen, X.; Li, L.; Jin, K.; Torkelson, J. M. Reprocessable polyhydroxyurethane networks exhibiting full property recovery and concurrent associative and dissociative dynamic chemistry via transcarbamylation and reversible cyclic carbonate aminolysis. *Polym. Chem.* **2017**, *8*, 6349–6355.
- (48) Smith, B., *Infrared spectral interpretation: a systematic approach*. CRC press: 2018, DOI: 10.1201/9780203750841.
- (49) Yuan, Q.; Zhou, T.; Li, L.; Zhang, J.; Liu, X.; Ke, X.; Zhang, A. Hydrogen bond breaking of TPU upon heating: understanding from the viewpoints of molecular movements and enthalpy. *RSC Adv.* **2015**, *5*, 31153–31165.
- (50) Yang, J.; Van Lith, R.; Baler, K.; Hoshi, R. A.; Ameer, G. A. A thermoresponsive biodegradable polymer with intrinsic antioxidant properties. *Biomacromolecules* **2014**, *15*, 3942–3952.
- (51) Akretche, H.; Pierre, G.; Moussaoui, R.; Michaud, P.; Delattre, C. Valorization of olive mill wastewater for the development of biobased polymer films with antioxidant properties using eco-friendly processes. *Green Chem.* **2019**, *21*, 3065–3073.
- (52) Anderson, J. M.; Hiltner, A.; Wiggins, M. J.; Schubert, M. A.; Collier, T. O.; Kao, W. J.; Mathur, A. B. Recent advances in biomedical polyurethane biostability and biodegradation. *Polym. Int.* **1998**, *46* (3), 163–171.
- (53) Du, P.; Liu, X.; Zheng, Z.; Wang, X.; Joncheray, T.; Zhang, Y. Synthesis and characterization of linear self-healing polyurethane based on thermally reversible Diels–Alder reaction. *RSC Adv.* **2013**, *3*, 15475–15482.
- (54) Cao, S.; Li, S.; Li, M.; Xu, L.; Ding, H.; Xia, J.; Zhang, M.; Huang, K. A thermal self-healing polyurethane thermoset based on phenolic urethane. *Polym. J.* **2017**, *49*, 775–781.
- (55) Mensor, L. L.; Menezes, F. S.; Leitão, G. G.; Reis, A. S.; Santos, T. C. d.; Coube, C. S.; Leitão, S. G. Screening of Brazilian plant extracts for antioxidant activity by the use of DPPH free radical method. *Phytother. Res.* **2001**, *15*, 127–130.
- (56) Brand-Williams, W.; Cuvelier, M.-E.; Berset, C. Use of a free radical method to evaluate antioxidant activity. *LWT—Food Sci. Technol.* **1995**, *28*, 25–30.